Development of thin elastomeric composite membranes for biomedical applications

S. H. TEOH, Z. G. TANG, S. RAMAKRISHNA
Institute of Materials Research and Engineering (IMRE), Centre for Biomedical Materials Applications and Technology (BIOMAT), Department of Mechanical and Production Engineering, National University of Singapore, 10 Kent Ridge Crescent, Singapore 119260

A breakthrough has been made in blending of two immiscible biocompatible polymers to form thin transparent interpenetrating network composite membranes (CM) with exceptional improvement in properties. Two immiscible polymers, namely the biaxially drawn ultra high molecular weight polyethylene (UHMWPE) film and polyether polyurethane (PU) were used. The fabrication included solution casting and heat compaction. During the fabrication, the CM still preserved the orientation of UHMWPE fibers but introduced the interpenetration of PU in UHMWPE film. The intimate interaction of PU with UHMWPE fibers was viewed through the transparency of CM. Differential scanning calorimetry (DSC) data showed the melting temperature (T_m) of UHMWPE increased by about 10 °C in CM and about 5 °C in heat-compacted membranes (HCM). Morphological observations indicated that CM presented a layered structure while HCM was a dense material without obvious void inclusions. The ultimate tensile strength and relative Young's modulus of CM are about 62 MPa and 460 MPa, respectively. They are about four times greater in strength and 150 times greater in modulus compared with those of PU. Heat compaction resulted in a membrane with nearly five times the tensile strength and 50 times the Young's modulus of PU. The engineered ultimate strain of CM is about 26%, 8% more than that of the porous UHMWPE film while about 70% of HCM, which is a 50% increase achieved through heat compaction. The tensile fracture toughness is about 93 mJ for CM and 211 mJ for HCM, two and five times that for the porous UHMWPE film, respectively. The significant modification on the properties of the heat-compacted composite may raise broad interest in using the CM to develop membrane-related devices and organ covers in biomedical applications.
© 1999 Kluwer Academic Publishers

1. Introduction

Elastomeric polymers have been widely used in medical applications for decades. They are found in artificial hearts, prosthetic heart valves, intra-aortic balloon pumps, mammary prostheses, opthalmological devices, maxillofacial restruction, artificial skin, and drug delivery systems [1, 2]. The primary types of elastomers used are silicone rubber and polyurethane. The success of polyurethane has increased the interest in more recent applications of polyurethane than silicone rubber, as disclosed in the surveys of both Leeper and Wright and McMillin's reviews [1, 2]. In the interest of its variety and tailor-made properties, polyurethane is considered as one of the promising candidate materials for this century's open issues, which are the development of small pore (less than 4 mm in diameter) vascular grafts [3, 4] and central flow flexible heart valve prostheses [5, 6].

However, polyurethane is plagued by progressive degradation when implanted. Degradation of the polyurethane [2, 7–13] has been extensively studied and categorized into proteolytic, hydrolytic, oxidative, radiation, and/or environmental stress inducing degradation. The implantable polyether urethanes are hydrolytically stable but subject to oxidative degradation in various forms, including metal ion oxidation (MIO), auto-oxidation (AO), and environmental stress cracking (ESC). Mechanisms of oxidative degradation are still unclear but strain-inducing scissors of the α position to the ether oxygen seem a source of failure for the medical products derived from polyether urethane elastomers.

Reducing the percentage of polyether moiety or completely removing it from polyurethane is considered as a practical way to increase the biostability of the implantable polyurethane. Efforts to achieve this have been found in either using poly(hexamethylene oxide) (PHMO), poly(octamethylene oxide) (POMO), and poly(decamethylene oxide) (PDMO) [14–16] or incorporating polycarbonate [13, 17] as macrodiol soft segments. The change of macrodiols incurs high cost on material selection, processing, and evaluation, especially, the assay of biocompatibility. Tang and coworkers suggested a new way of composite processing by incorporation of a highly porous biaxially drawn ultra-high-molecular-weight polyethylene (UHMWPE) with polyether urethane [18, 19]. The primary objective

is to differentiate the mechanical load from amorphous polyurethane to the semicrystalline UHMWPE reinforcement. The significance of this coupling was addressed on the simplicity of processing and the excellent biocompatibility of the employed materials. No compatibilizer was used in the composite fabrication.

Theoretically the blend of two immiscible polymers hardly achieves a homogenous phase and improved properties if no compatibilizer is used. Compatibilizers are often considered as a problem for the biocompatibility of medical polymers. Composite blend derived from the suggested biaxially drawn UHMWPE and PU is viewed as a significant contribution in the development of new generation biomaterials [20]. Our interest in fabrication of composite membranes (CM) using the biaxially drawn UHMWPE and polyurethane was initiated by the discovery of an optical clear UHMWPE (biaxially drawn)/polyurethane composite [21]. Strong and flexible thin transparent composite membranes with unusual properties can be developed through composite processing of the biaxially drawn UHMWPE and PU.

The exceptional mechanical strength and modulus of flexible chain polymers like polyethylene can be achieved by drawing [22]. Currently there are two types of commercialized drawn UHMWPE available, which are uniaxially drawn UHMWPE, (e.g. Spectra supplied by Allied Signal, Inc, USA) and biaxially drawn UHMWPE (e.g. Solupor from DSM, the Netherlands). Uniaxial drawing makes UHMWPE a stiffer and stronger polymer, which has a tensile strength of approximately 6 GPa and a modulus of 220 GPa, compared to those of steel. While the biaxially drawn UHMWPE films displayed a tensile strength up to 600 MPa and a modulus up to 10 GPa [23, 24]. The impressive mechanical properties of uniaxially drawn UHMWPE have been extensively exploited in fabrication of composites. Typical applications include helmet, denture, and orthodontic brackets [25, 26]. However, the biaxially drawn UHMWPE films are not frequently reported because of the lower significance on mechanical properties.

The fine fiber mesh and highly porous structure of biaxially drawn UHMWPE films [27, 28] enhance the possibility of composite blending of two immiscible polymers. The fibers are small and have a diameter down to approximately 100 nm. The porosity of the films is approaching 90% through a controlled drawing process. The incorporation of these nanofibers with elastomers such as polyurethane is of interest in academic study and applications, especially biomedical applications.

In this paper, we report the processing conditions, optical properties, thermal properties, morphology and fracture morphology, and tensile properties of the thin CM. Correlation of morphology and mechanical properties is also attempted.

2. Materials and methods

2.1. Materials

Biaxially drawn UHMWPE films (Solupor^{TM} 7P03) were used as the reinforcement material for fabrication of composite membranes. They were purchased from DSM Solutech BV, the Netherlands, and have a thickness of 35 μm and a porosity of 78%. The selection of this UHMWPE fabric is attributed to its high porosity of this semicrystalline fibrous polymer, its ultrafine structure, and its availability in the form of large films.

The polymer matrix is a polyether polyurethane, Toyobo® TM5. It was kindly provided by Toyobo Co., Osaka, Japan. The soft segment is composed of polytetramethylene glycol (PTMG) and 4,4′-diphenylmethane diisocyanate (MDI) while the hard segment contains propylene diamine and MDI. The designed TM series include, TM1, TM3, and TM5, which are derived from the soft segment macrodiols of molecular weights of 850, 1350, and 2000, respectively. The mechanical properties of these polyurethanes have been published previously [29–31]. Toyobo® TM5 is similar to Biomer® (Ethicon Inc., Somerville, USA). After the withdrawal of Biomer® from medical applications, it was considered as one of the alternatives in medical applications [2].

Generally polyurethanes have a solubility ranging from 18.3 to 26.5 $MPa^{1/2}$. Toyobo® TM5 is similar to Biomer, which has a solubility parameter of 21.4 $MPa^{1/2}$ for soft type and 26.5 $MPa^{1/2}$ for hard type. Typical solvent used for Toyobo® TM series is *N*,*N*′-dimethyl formamide (DMF). It has a solubility parameter of 24.7 $MPa^{1/2}$ and was selected as the carrier solvent for fabrication of the composite membranes. A solution of 10% Toyobo® TM5 was dissolved in DMF and used as the starting solution for penetrating into UHMWPE membrane.

2.2. Methods

2.2.1. Fabrication of CM

The experimental set-up for fabrication of CM consists of three parts. They are impregnation, vacuum drying, and heat compaction (Fig. 1). The impregnation process includes an impregnation chamber, drying agent, and a desiccator. UHMWPE film fixed in a frame fixture was placed in the impregnation chamber full of polyurethane/DMF solution. Dry agent (silicone gel) was used to maintain a proper humidity in the desiccator. After a definite time (the scheduled time ranged from 5 to 200 h), the polyurethane wetted UHMWPE film was transferred to the drying chamber for vacuum drying. The drying

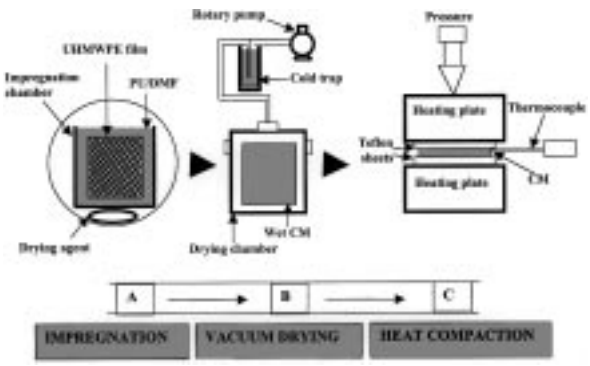

Figure 1 Schematic diagram of the experimental set-up for the preparation of CM. (A) Impregnation; (B) vacuum drying; (C) heat compaction.

chamber was conditioned at a definite temperature (the temperature was conditioned from 30 to 80 °C) and a vacuum pressure of 740 mmHg for a period until the composite membrane approached a constant weight. The vacuum drying system consists of a drying chamber, cold trap, and rotary pump. Liquid nitrogen was used as the cooling agent for the protection of the rotary pump from solvent attack. After vacuum drying, a composite membrane was obtained. The composite membrane was heat compacted in Laboratory Presses (LABQUIP Model LP 50, Lab Tech Engineering Company, Ltd) at temperatures from 110 to 140 °C under a pressure of 18 MPa for 1.5 h. For ease of handling, Teflon sheets were used for heat compaction. To monitor the exact temperature between Teflon sheets, a thermocouple (T-Copper Constantan Model 199, Omega) was placed inside the Teflon sheets during the process. The heat-compacted composite membrane (HCM) was removed from the Teflon sheets upon cooling to room temperature.

The fabrication conditions were optimized by visually inspecting the opaque defects on the final drying transparent CM produced. A two-dimensional fabrication diagram was drawn based on the impregnation time and drying temperature (Fig. 2). Fig. 2 indicates a zone of compromise between impregnation time and drying temperature. To obtain a transparent composite membrane with the least influence on the properties, 72 h impregnation and 40 °C drying temperature were appropriate, as indicated in Fig. 2.

Heat compaction was used to remove the voids in CM created by solution casting. Temperature for heat compaction was studied from 110 to 140 °C. A heat compaction conducted at a temperature up to 125 °C, is the best as it reserved the crystalline structure of UHMWPE and also maximally removed the voids in the CM.

2.2.2. Light transmission

Light transmission tests of membranes were performed on a U-3410 Spectrophotometer (Hitachi). The aperture for light transmission is 10 × 10 mm and the wavelength of the light was fixed at 600 nm. Light transmission rate was obtained for the effect of processing on the transparency of specific materials.

2.2.3. Polarized light transmission

A polarized light microscope (Nikon, Optiphot-pol, Japan) was used to study the orientation of UHMWPE fibers in UHMWPE film, CM, and HCM. Transparent CM were mounted directly on to the sample stage while the UHMWPE film was immersed into a refractive index (about 1.55) matching immersion oil before observation. The magnification was calculated using standard grating plates for comparison.

2.2.4. Differential scanning calorimetry (DSC)

The thermal history of materials was recorded using DSC. DSC experiments were conducted using DSC-200 Netzsch scanning calorimeter calibrated with an indium standard. Discs of each material weighing approximately 2 mg were placed in an aluminum sample pan, and thermograms were recorded in a temperature between 40 and 200 °C at a heating rate of 5 °C min^{-1}.

2.2.5. Tensile test

Mechanical properties of UHMWPE film, CM, HCM, and PU were evaluated using an Instron testing machine (Model 5566 with 1 kN load cell) and analyzed in accordance with ASTM D882-91 standard test protocol for thin film tensile tests. Specimens were made 75 mm long and 10 mm wide. For ease of handling these fragile specimens, paper frame fixtures were used (Fig. 3). Pneumatic grips were employed to avoid specimen slippage during test. All the tests were conducted at a crosshead speed of 5 mm min^{-1} under controlled temperature at 23 ± 1 °C and relative humidity of 50 ± 5%.

Special care was taken on the thickness measurement of ultrathin films. Unlike one-point contact thickness measurement for hard materials, a large contact area was needed for measuring the thickness of soft membrane. A modified method for thickness measurement was carried out on a one-point contact instrument (Cary Compar B). A standard 1.000 mm thick plate was used and put on top of the specimen (Fig. 4).

The grip separation distance was set at 50 mm. The engineering stress (σ is defined as the ratio of the load

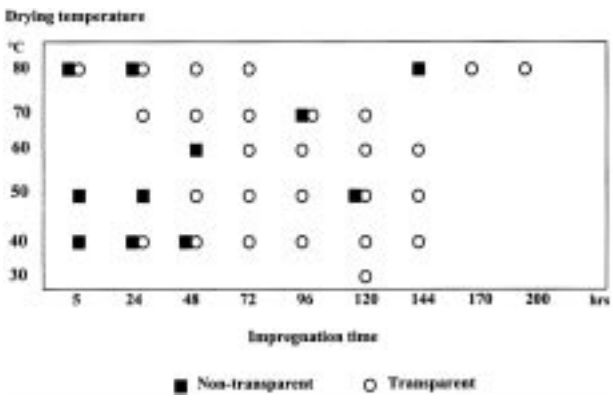

Figure 2 2-D fabrication diagram based on impregnation time and drying temperature ($n = 38$).

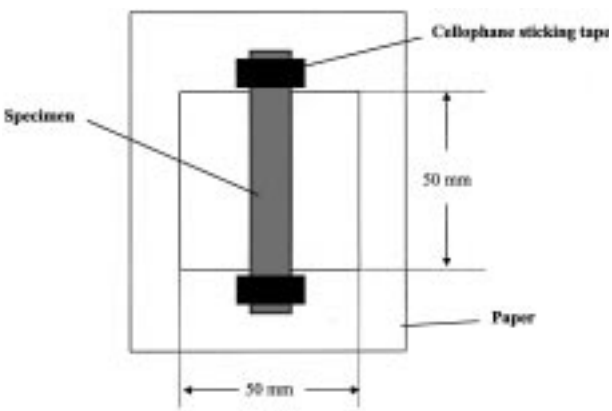

Figure 3 Paper frame for specimen fixation in the tensile tests.

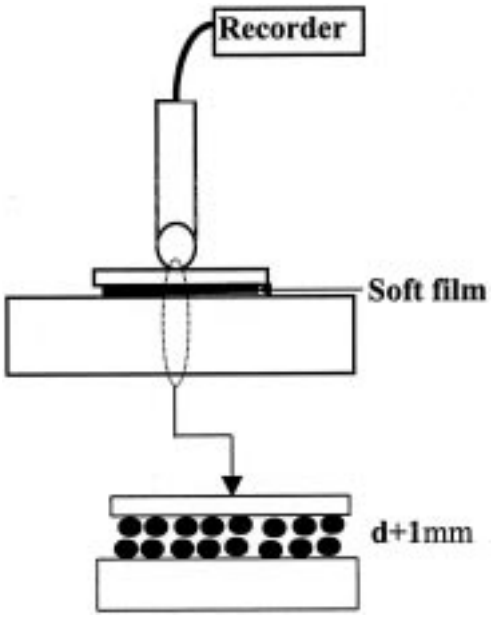

Figure 4 Schematic set-up for thickness measurement. The dashed line elliptical areas are amplified to show the mechanism of the tests.

(L) to the area (A)), ($\sigma = L/A, A = w \times t$, where w is the specimen width (10 mm) and t is the thickness). The percentage strain (λ) is, $= [(l - l_0)/l_0] \times 100\%$, where l is the total extension measured from the grip displacement and l_0 is the gage length (25 mm). The relative modulus (E) was calculated from the initial slope of the stress–strain curve obtained. The tensile toughness is the product of the stress and strain revealed in the typical stress–strain curve or work done during test processing to the fracture strain. The tensile strength was recorded as the stress at the ultimate fracture.

2.2.6. Scanning electron microscopy (SEM)

All specimens were examined in transverse and/or longitudinal sections. Specimens for transverse observations were made either by freeze cutting in liquid nitrogen or fracture after tensile tests. Specimens for longitudinal observations were used directly or fabricated by peeling the membrane into two parts for detection of the inner layer morphology. All the specimens were coated with gold for morphological observations. Pictures were taken from the SEM machine (Jeol JSM-T330 scanning microscope). The working voltage used was either 5 kV or 10 kV. Lower voltage is encouraged for preservation of fine details of UHMWPE specimens [32].

3. Results

3.1. Optical properties

The UHMWPE film is highly porous and opaque. When impregnated with polyurethane, it becomes transparent (Fig. 5). The optical clearance of CM indicated the good refractive index matching of the component materials. The refractive index of UHMWPE is approximately 1.545 [33]. The difference of refractive indices between UHMWPE and polyurethane, to the maximum, is approximately 0.1 (refractive indices for the polyurethane family ranges from 1.50 to 1.65) [34].

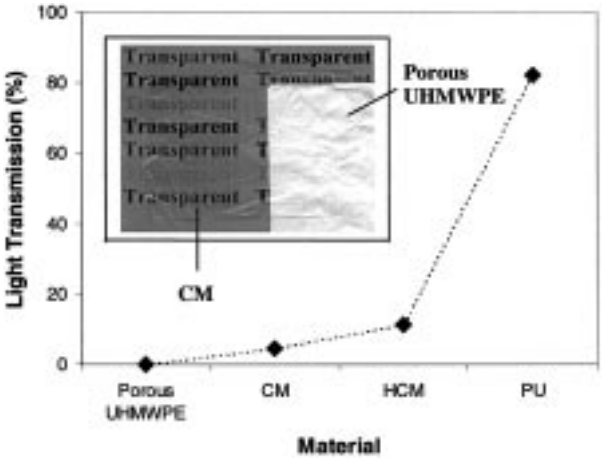

Figure 5 The transparency of CM viewed at 600 nm wavelength. The photo shows visual transparency of the CM. The opaque film is the porous UHMWPE film for comparison. The plot shows the light transmission of the porous UHMWPE film for CM, HCM and PU.

The transparencies of UHMWPE film, CM, and polyurethane were measured in light transmission rate (Fig. 5). Light transmitted through CM indicated that the sizes of air bubbles or voids are much smaller than the wavelength of the light [35]. Heat compaction had a significant impact on the light transmission. The light transmission rate of HCM is approximately 10% and twice that of CM. It indicated a further removal of voids or reducing the size of voids in CM was achieved through heat compaction. To achieve higher light transmission rate like PU, precise matching of refractive indices of UHMWPE and PU is needed [36].

3.2. Polarized light transmission

Results from optical polarized light microscopy indicated that composite processing and heat compaction have not significantly altered their fiber orientations (Fig. 6). However, disturbance of the orientations was found when the relative angle between fibers from two perpendicular directions was measured (Fig. 6, Table I). The relative angle θ indicated an insignificant change

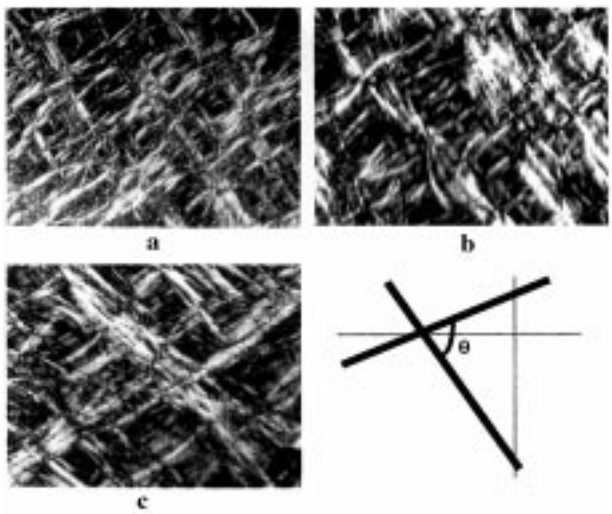

Figure 6 Polarized light micrographs (× 500) of the porous UHMWPE film (a), CM (b) and HCM (c). Fiber orientation in all membranes was measured in the relative angle shown.

TABLE I Relative angle between fibers from different directions

Material ($n = 3$)	Relative angle θ and standard deviation (degree)
UHMWPE film	91 ± 1
CM	88 ± 9
HCM	85 ± 7

in CM but the standard deviation significantly increased in both CM and HCM compared with UHMWPE film. In addition, the fibers in CM have a size more than double that in UHMWPE film and the uniformity of the fibers was also reduced after impregnation and heat compaction.

3.3. Differential scanning calorimetry

The DSC curves of UHMWPE film, CM, HCM and PU are shown in Fig. 7. The temperatures of the endothermic peaks and the corresponding heats of fusion are listed in Table II. Crystallinity of the UHMWPE in UHMWPE film and CM is calculated based on a crystallinity heat of fusion of 293 J g^{-1} [37] and the fiber fraction in CM (25–40%). The DSC curves of the materials indicated that composite processing has changed the melting behavior of the UHMWPE component in CM. Solution casting shifted the T_m of UHMWPE film from 138 to 147 °C (approximately 9 °C increase). Heat compaction annealed the composite at 125 °C and partially released the tension of the fibers. The T_m of the HCM still gained an increase of about 6 °C. Composite processing also introduced a slight decrease in the crystallinity of UHMWPE semicrystalline structure.

3.4. Tensile test

The tensile properties of UHMWPE film, CM, HCM and PU are summarized in Table III. The incorporation of polyurethane into UHMWPE film has a significant impact on the tensile properties of the CM. The ultimate tensile strength of CM is 62 ± MPa. It is about four times that of PU. The ultimate tensile strength of HCM is 80 ± 1 MPa. It is about five times that of PU. Both CM and HCM have enhanced mechanical properties compared with PU. HCM gained the high tensile strength

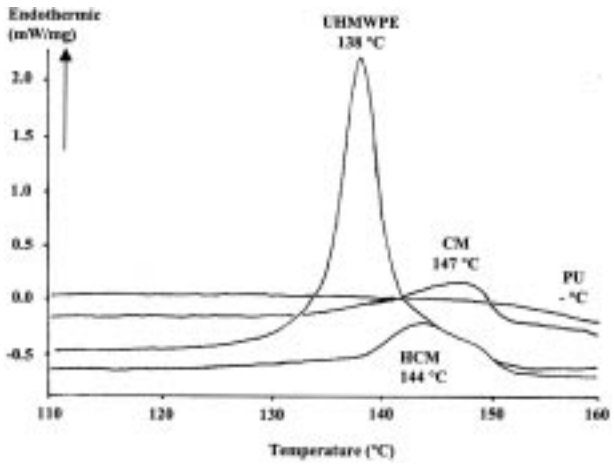

Figure 7 The thermal behavior of the drawn UHMWPE film (137 °C), CM (147 °C), HCM (144 °C) and PU from 40 to 200 °C.

TABLE II DSC results of the drawn UHMWPE, HCM, CM and PU

Material	T_m (°C)	Heat of fusion (J g^{-1})	Crystallinity estimated (%)*
Drawn UHMWPE film	138	185	63
CM	147	39	33 ~ 54
HCM	144	36	31 ~ 50
PU	—	—	—

*Based on a crystalline heat of fusion of 293 J g^{-1}. The crystallinity of CM was calculated based on the net UHMWPE mesh incorporated (fiber fraction was about 25 to 40%).

TABLE III Tensile properties of reinforcement, matrix and CM ($n = 5$)

Material	Strength (MPa)	Strain (%)	Young's modulus (MPa)	Tensile toughness (mJ)
UHMWPE film*	49 ± 4	18 ± 1	314 ± 31	42 ± 7
PU	17 ± 2	1295 ± 53	3 ± 0.2	2469 ± 10
CM	62 ± 4	26 ± 2	460 ± 63	93 ± 4
HCM	80 ± 1	69 ± 5	61 ± 4	211 ± 28

*UHMWPE film is a porous material and the tensile properties tested based on the thickness of the porous film using the defined method in Fig. 4.

through combined treatment of solution casting and heat compaction. Heat compaction cast a great effect on the ultimate strain of CM when compared with the reinforcement UHMWPE. The engineered ultimate strains of CM and HCM are 26 ± 2% and 69 ± 5%, respectively. These are about two and four times that of UHMWPE film. Better interaction of UHMWPE film with polyurethane was found in HCM. Fig. 8 shows the typical stress–strain curves of UHMWPE film, CM, HCM and PU. After impregnation of polyurethane, the relative modulus of the CM is increased. It is about 180 times that of PU. CM also shows a greater tensile toughness compared with the UHMWPE film. It is about twice that of the UHMWPE film. After heat compaction, the modulus of HCM is decreased because of the annealing process at 125 °C. It is about half that of the porous UHMWPE film but still about 50 times that of PU. The tensile toughness of HCM is significantly improved compared with the UHMWPE film. It is about five times that of the UHMWPE film. It indicated a good interaction of UHMWPE with PU.

3.5. Scanning electron microscopy

SEM studies show that the surface of the UHMWPE film is highly porous (Fig. 9a). The biggest pore ranges from 50 to 100 μm. When impregnated with polyurethane, the UHMWPE film loses the porous structure and becomes a dense material, the surface of UHMWPE film is covered by a smooth defect free polyurethane layer. The inner layers of UHMWPE film were also well impregnated with PU (Fig. 9b). Texture of fibers was detected on the surface of peeled-off samples specially made from two UHMWPE films. The cross-section of the UHMWPE film is a loose layered structure (Fig. 10a). When impregnated with PU, both the inner layers and surface layers of UHMWPE film are drenched with PU solution.

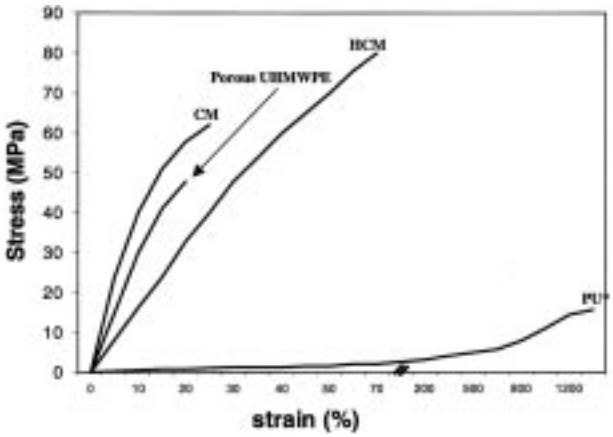

Figure 8 Typical tensile properties of the porous UHMWPE film, PU, CM and HCM. Note: PU curve was drawn in a compact way and did not follow the standard scales for the UHMWPE film, CM and HCM ($n = 5$).

After vacuum drying, PU was frozen in the form of interpenetrating networks on the scaffolds of the fibers in the porous UHMWPE film (Fig. 10b). HCM shows a single non-layered condensed structure (Fig. 10c). Voids in HCM were removed through a heat compaction process.

The fracture surface morphologies of the UHMWPE film and CM were completely different. The fracture of UHMWPE film initiated at the weak point of the pores, then propagated along the direction of the stress concentration until it approached the coarse fibers (Fig. 11a). The fine fiber mesh was contracted when the fracture developed along the coarse fibers. At the same time, the coarse fibers began to align along the direction of the external stretching. The fracture of coarse fibers therefore became the dominant phenomena. During stretching, macro-necking of UHMWPE film occurred all the time. At the ultimate point of fracture, pull-out of coarse fibers dominated the cross-section of the fractured UHMWPE film samples (Fig. 11a). In CM, the fine fiber mesh of UHMWPE was frozen in PU layers, voids were filled with PU and the weak point shifted from the large pores of the porous UHMWPE film to smaller pores at the junction between the fine fiber mesh and coarse fibers. The fracture of CM initiated at these conjunctions and propagated along the coarse fibers. Unlike UHMWPE film, the fine fiber mesh/PU composite adhered on the neighboring sublayers held strongly by the interpenetration of PU (Fig. 11b). No necking was seen in the fracture of CM. Instead of necking, the samples of CM became stress whitened when the strain approached the point of the fracture of the UHMWPE film. The stress whitening of the samples increased gradually until fracture occurred; this is a result of the presence of voids which scatter light in the deformed specimens [38, 39].

The fracture surface of the CM shows the interconnection and random rupture of the composite layers. These clearly indicated the interpenetration of PU in the CM (Fig. 11b). The HCM shared the same characteristics as the CM, but differences still existed in the consolidation of the fine fiber mesh and coarse fibers. The UHMWPE fine fiber mesh was well impregnated with PU and its connection with coarse fibers is stronger than that in CM (Fig. 11c). Voids have almost been depleted. It resulted in better mechanical properties of HCM. The high ultimate strength of HCM left a semicircular shape of the fracture course after fracture (Fig. 11c).

4. Discussion

Conventionally, melt process is the predominant method for fabrication of thermoplastic polymers, composites, and blends [40–42]. In composite fabrication, melt process requires the matrix polymer of a lower melting temperature than that of the reinforcement fabric for the preservation of the strength of fabric. The low melting temperature of UHMWPE film limited the application of this melt process in UHMWPE and PU system. Solution casting is therefore a practical method for fabrication of UHMWPE/PU composite membranes. As it is well known, the wettability of polar PU with non-polar polyethylene is very low. Interaction of PU with UHMWPE film becomes the key issue for solution casting process. Interpenetrating PU thorough the UHMWPE film is the primary concern in our fabrication.

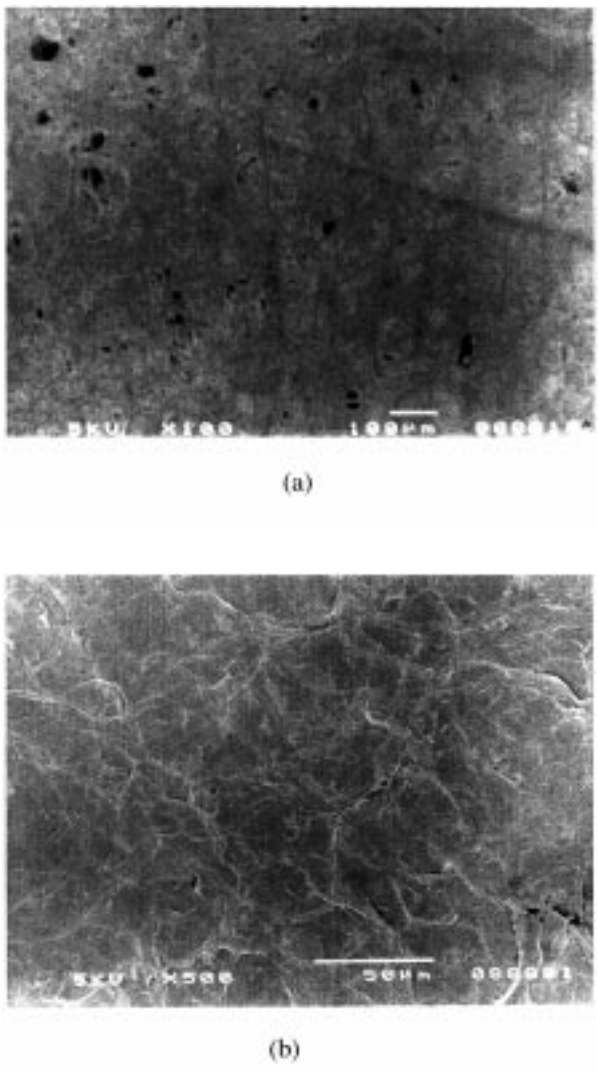

Figure 9 Surface views of the UHMWPE film (a) and peeled off from the CM (b).

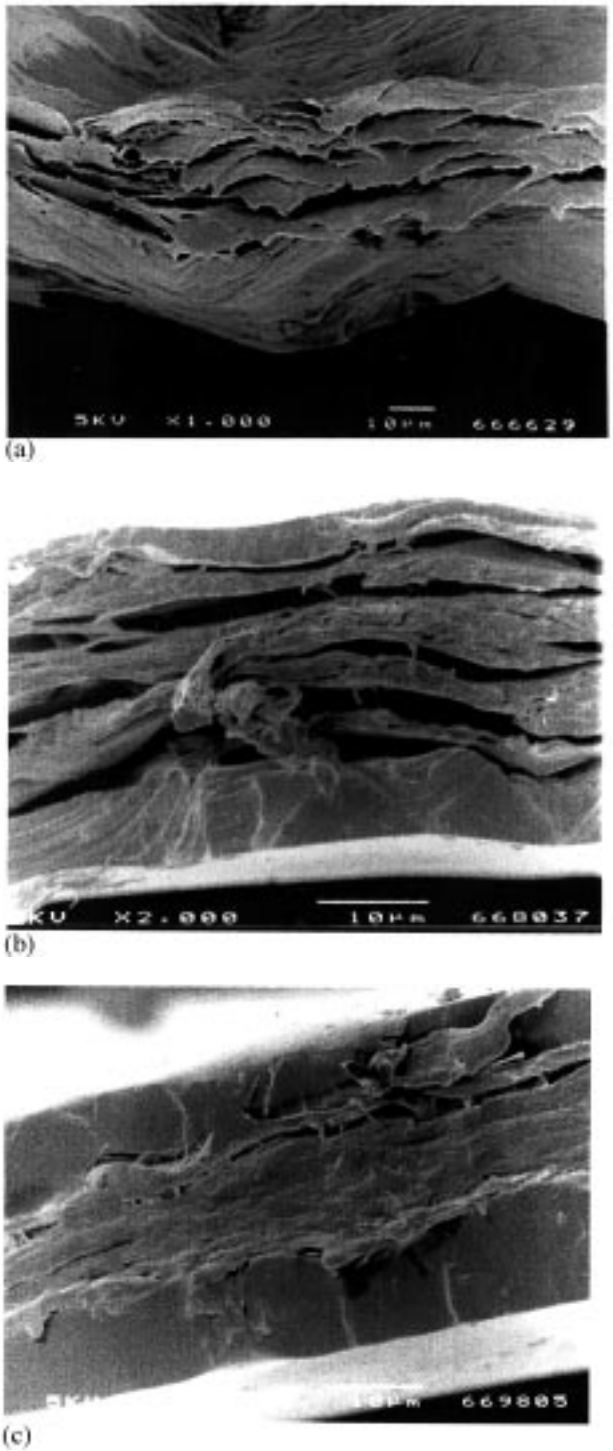

Figure 10 Cross-section view of UHMWPE film (a), CM (b) and HCM (c).

The highly porous UHMWPE thin film was selected for the ease of penetration of PU and solvent removal. Polyethylene is inert to many solvents. Incorporation of the strength of the drawn UHMWPE is not a problem in the solution casting process but engineering the flexibility of PU to UHMWPE is questioned. The mechanical properties of HCM indicated a good interaction of UHMWPE with PU. Both the tensile strength and strain are significantly enhanced (Fig. 8). It is interesting to elaborate the extent of interaction of polyurethane with UHMWPE in both CM and HCM.

Penetration of PU through UHMWPE film is the microscale interaction between PU and UHMWPE. The UHMWPE film has an average pore size of approximately 300 nm and a pore size distribution from 200 to 400 nm (Coulter method, ASTM E1294-89). The large pores were discernible and have a pore size up to 100 µm (Fig. 9). These pores are the channels for the polyurethane DMF solution wetting the inner layers of UHMWPE film. The solution was spread along the surface of each sublayer of the UHMWPE film. It was driven by the capillary effect of the huge surface created from the biaxial drawing process. During the impregnation, the opaque UHMWPE film becomes translucent due to the refractive index matching of PU solution and the depletion of air bubbles in the porous structure. When vacuum dried, the surface layers of PU were dried and formed thin PU membranes on the UHMWPE film. The

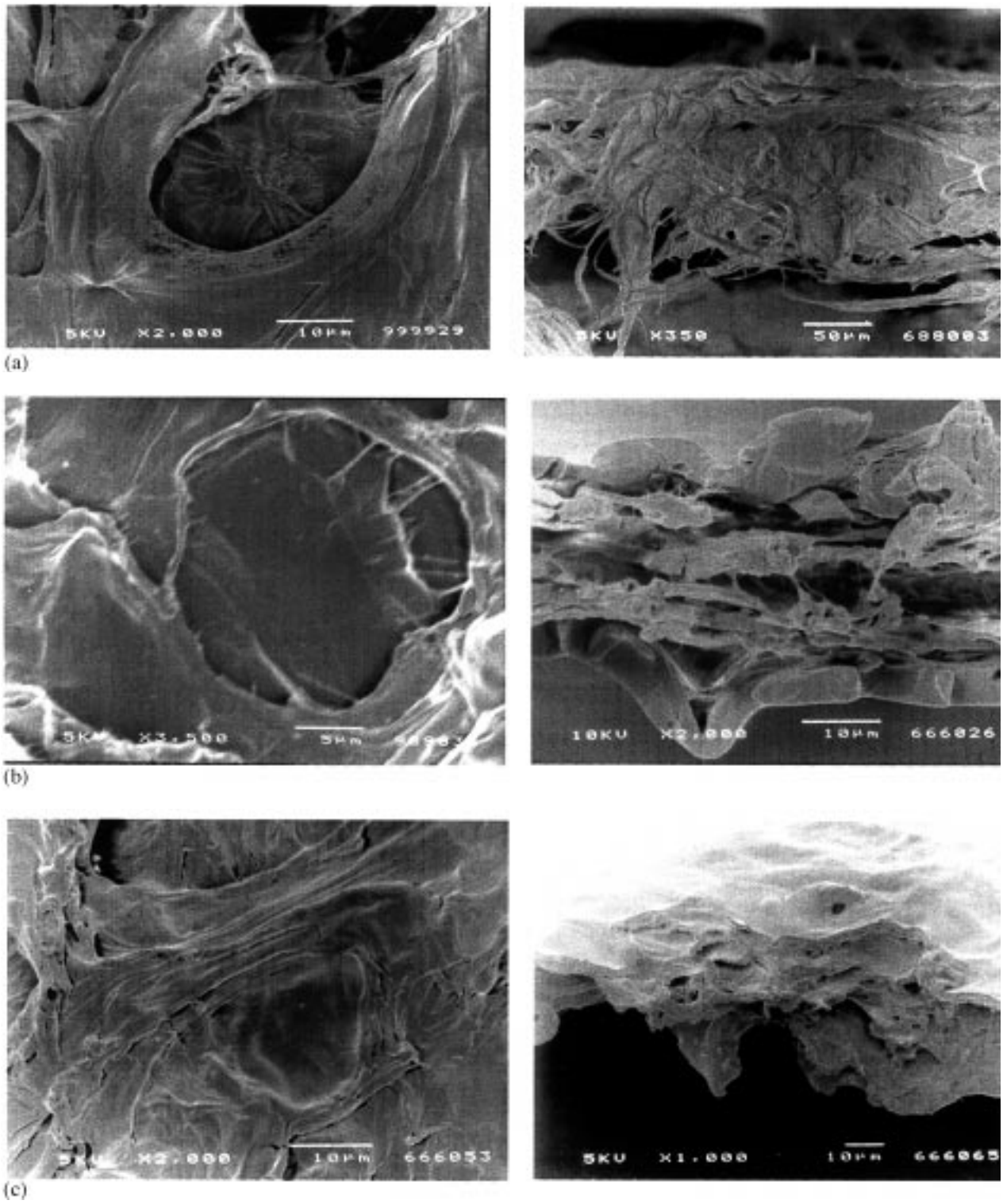

Figure 11 Fracture morphologies of UHMWPE film (a), CM (b) and HCM (c).

residual DMF was squeezed out by the pressure difference between inner layer and surface layer until the CM approached a constant weight. The CM becomes transparent with the depletion of the residual DMF. The interconnection associated with interpenetration of PU was also seen in the polarized light transmission photography. The large disturbance of fiber orientation implied the existence of irregular penetrations derived from different pore size formulations (Fig. 6 and Table I). The surface view of the inner layer in CM shows a thorough impregnation of UHMWPE with PU (Fig. 9). The thorough impregnation of UHMWPE film was also verified in the fracture morphology of CM (Fig. 11). The fracture courses were changed after the incorporation of PU with UHMWPE.

The thorough impregnation of PU with UHMWPE can further be seen from the optical properties of CM (Fig. 5). According to Willmouth [35] the transparency of CM would not be achieved if air bubbles of a diameter up to 300 nm exist. The discernible gaps (in microscale) between sublayers in CM could not be the air inclusion but the voids after depletion of DMF. Otherwise, such a gap of unwettability would be revealed as haze in the CM. The transparency of the CM is the contribution of

the transparency of the composite sublayers. Interesting data were found in light transmission of the membrane materials. UHMWPE is opaque and the light transmission rate approaches zero. The interconnecting porous structure in UHMWPE film is the primary reason for the light scattering other than light transmission. When incorporated with PU, the porosity of UHMWPE film is reduced and about 5% of light transmitted through the CM. The interpenetration of PU in the UHMWPE film is obvious otherwise the transparency of CM could not be achieved. Heat compaction reveals the possibility of obtaining higher light transmission rate. It can eliminate the gas inclusions and also enable the refractive index matching when UHMWPE and PU interact with each other under internal and external pressure and high temperature [43].

A mechanism of molecular blending between amorphous UHMWPE molecules with amorphous PU moiety is proposed based on the thermal properties of both CM and HCM. The microscale interaction of uniaxially drawn fibers with polymer matrix has no significant effects on the thermal properties of crystalline fibers. When biaxially drawn UHMWPE was used as reinforcement material, significant influence was found in the melting behaviors of UHMWPE in CM. The T_m of UHMWPE increased by approximately 10 °C which could not be credited to the overheating through high heat rate because the heating rate is set low at 5 °C min^{-1}. The increase of T_m of UHMWPE could not also be credited to the surface coating of the thin PU membrane because the control test already excluded the possibility of this effect. DMF impregnation has no effects on the T_m of UHMWPE film. When annealing the CM at 125 °C, the T_m of UHMWPE was dropped to approximately 143 °C with a significant decrease of crystallinity. It indicated that the higher the crystallinity the higher the melting point. UHMWPE is a semicrystalline polymer. The melting point of the perfect single crystal is decreased when miscible amorphous phase coexisted. The melting point of UHMWPE film actually is the melting range of the binary phase UHMWPE. According to the heat of fusion, UHMWPE film has a crystalline phase of approximately 63.2% and an amorphous phase of approximately 36.8%. When impregnated with PU, PU can partially swell the extended amorphous UHMWPE chains because the soft polyether moiety has a solubility parameter in the range of 16.3 $MPa^{1/2}$ to 18.3 $MPa^{1/2}$ and is sufficient to swell amorphous UHMWPE chains in CM. The introduction of PU moiety into amorphous UHMWPE chains reduced the amount of the miscible components in the UHMWPE binary system and also created a molecular repulsion between polar and non-polar molecules. The T_m in CM, therefore, significantly increased. Significant changes to the unit cell of UHMWPE as revealed by wide angle X-ray have been detected and this will be reported in another publication.

In summary, the interaction of PU with UHMWPE film is on the molecular level between amorphous PU and polyethylene and in nanoscale between amorphous PU and crystalline UHMWPE, forming interpenetrated network composites. The transparency of CM increased with the decrease of the gaps between the sublayers. Heat compaction maximally eliminated the gaps and merged the sublayers of CM. Mechanical properties of CM are significantly improved when heat compaction was used.

5. Conclusions

A breakthrough in making transparent elastomeric CM was achieved through the combination of biaxially drawn porous UHMWPE and PU, two immiscible polymers without any compatibilizer. The porous structure of the drawn UHMWPE film encouraged the impregnation of polar PU. Through controlled processing, the coexistence of UHMWPE and PU was achieved resulting in an interpenetrated network composite. The molecular level of blending between PU and amorphous UHMWPE and the nanoscale composite between crystalline UHMWPE and PU or PU/amorphous UHMWPE blend contributed significantly to the optical properties of CM. Maximum increase on tensile strength and strain were obtained through the optimized heat compaction process. The molecular blending and nanoscale composite processing raise a great interest in characterization of the intimate interaction of reinforcement material and matrix polymer, which may be immiscible or partially miscible. Since UHMWPE and PU are biocompatible materials, the CM are of significant promise in biomedical applications, especially in tissue engineering consideration where strength of the thin films is a concern.

Acknowledgment

The authors would like to thank Professor Mitso Umezu, Waseda University, for his help in getting the PU and thanks also to Toyobo Co., Osaka, Japan for kindly supplying the Toyobo TM5 material. The authors also would like to thank Dr K. T. Tsai, Instron Singapore Pte Limited for his assistance in arranging the tensile tests.

References

1. H. M. LEEPER and R. M. WRIGHT, *Rubber Chem. Technol.* **56** (1983) 523.
2. C. R. MCMILLIN, *ibid.* **67** (1994) 417.
3. E. PARIS, M. W. KING, R. G. GUIDOIN, J.-M. DELORME, X. DENG and Y. DOUVILLE, in ''Polymeric biomaterials,'' edited by S. Dumitriu (Marcel Dekker, Inc., New York, 1994) p. 245.
4. M. SZYCHER, in ''Blood compatible materials and devices: perspectives towards the 21st century,'' edited by C. P. Sharma and M. Szycher (Technomic Publishing Co., Inc. Lancaster, PA 1991) p. 33.
5. J. JANSEN, S. WILLEKE, B. REINERS, P. HARBOTT, H. REUL, H. B. LO, S. DABRITZ, C. ROSENBAUM, A. BITTER, K. ZIEHE, G. RAU and B. J. MESSMER, *ASAIO Trans.* **37** (1991) M451.
6. T. G. MACKAY, G. M. BERNACCA, A. C. FISHER, C. S. HINDLE and D. J. WHEATLEY, *Artif. Org.* **20** (1996) 1017.
7. H. J. GRIESSER, *Polym. Degradation Stability* **33** (1991) 329.
8. W. LEMM, in ''Polyurethane in biomedical engineering,'' edited by H. Planck, G. Egbers and I. Syre (Elsevier Science, Ansterdam 1984) p. 103.
9. M. A. SCHUBERT, M. J. WIGGINS, J. M. ANDERSON and A. HILTNER, *J. Biomed. Mater. Res.* **34** (1997) 319.
10. M. A. SCHUBERT, M. J. WIGGINS, M. P. SCHAEFER, A. HILTNER and J. M. ANDERSON, *ibid.* **29** (1995) 337.

11. K. STOKES, R. MCVENES and J. M. ANDERSON, *J. Biomater. Appl.* **9** (1995) 321.
12. K. B. STOKES, A. W. FRAZER and E. A. CARTER, ANTEC' 1984, The Society of Plastics Engineers, Inc. 42nd Technical Conference, April 30-May 3, New Orleans, LA, pp. 235–244.
13. M. SZYCHER, A. M. REED and A. A. SICILIANO, *J. Biomater. Appl.* **6** (1991) 110.
14. D. J. MARTIN, G. F. MEIJS, G. M. RENWICK, S. J. MCCARTHY and P. A. GUNATILLAKE, *J. Appl. Polym. Sci.* **62** (1996) 1377.
15. D. J. MARTIN, G. F. MEIJS, G. M. RENWICK, P. A. GUNATILLAKE and S. J. MCCARTHY, *ibid.* **60** (1996) 557.
16. D. J. MARTIN, G. F. MEIJS, P. A. GUNATILLAKE, S. J. MCCARTHY and G. M. RENWICK, *ibid.* **64** (1997) 803.
17. M. C. TANZI, D. MANTOVANI, P. PETRINI, R. GUIDON and G. LAROCHE, *J. Biomed. Mater. Res.* **36** (1997) 550.
18. Z. G. TANG, S. RAMAKRISHNA and S. H. TEOH, in ''9th International Conference on Biomedical Engineering,'' 3–6 December 1997, Singapore, p.563.
19. S. H. TEOH and Z. G. TANG, Keynote Lecture, Symposium on Emerging Plastics Technologies into the New Millenium, Malaysian Plastics Manufacturers Association (MPMA) 3–5 Nov. 1997, Petaling Jaya, Selangor Darul Ehsan, Malaysia.
20. A. J. JONES and N. T. DENNING, (eds), in ''Polymeric biomaterials, bio- and eco-compatible polymers, a perspective for Australia'' (Department of Industry, Technology and Commerce, Australia, 1988).
21. S. H. TEOH, Z. G. TANG and S. RAMAKRISHNA, Singapore Patent Application No 9702630-6, 25 Aug. 1997.
22. R. S. PORTER, T. KANAMOTO and A. E. ZACHARIDES, *Polymer* **35** (1994) 4979.
23. N. S. J. A. GERRITS, R. J. YOUNG and P. J. LEMSTRA, *ibid.* **31** (1990) 231.
24. Y. SAKAI, K. UMETSU and K. MIYASAKA, *ibid.* **34** (1993) 318.
25. Y. Y. CHENG, T. W. CHOW and N. H. LADIZESKY, *J. Macromol. Sci.–Phys.* **B32** (1993) 433.
26. P. D. COATES, G. R. DAVIES, R. A. DUCKETT, A. F. JOHNSON and I. M. WARD, *Trans. Int. Chem. E.* **73** (1995) 753.
27. N. S. J. A. GERRITS and P. J. LEMSTRA, *Polymer* **32** (1991) 1770.
28. Y. SAKAI and K. MIYASAKA, *ibid.* **29** (1988) 1608.
29. K. HAYASHI, H. TAKANO, T. MATSUDA and M. UMEZU, *J. Biomed. Mater. Res.* **19** (1985) 179.
30. K. HAYASHI, T. MATSUDA, H. TAKANO and M. UMEZU, *ibid.* **18** (1984) 939.
31. K. HAYASHI, T. MATSUDA, T. NAKAMURA, M. UMEZU and H. TAKANO, in ''Progress in Artifical Organs,'' edited by Y. Nose, C. Kjellstrand and P. Ivanovich (ISAO Press, Cleveland, 1986) p. 989.
32. D. PIENKOWSKI, R. JACOB, D. HOGLIN, K. SAUM, H. KAUFER and P. J. NICHOLLS, *J. Biomed. Mater. Res.* **29** (1995) 1167.
33. J. BRANDRUP and E. H. IMMERGUT (eds), ''Polymer handbook,'' 2nd edition (John Wiley & Sons, Inc., New York, 1975).
34. S. H. TEOH, Z. G. TANG and G. W. HASTINGS, in ''Handbook of biomaterial properties,'' edited by J. Black and G. Hastings (Chapman & Hall, London, 1998) p. 270.
35. F. M. WILLMOUTH, in ''Optical properties of polymers,'' edited by G. H. Meeten (Elsevier Applied Science Publishers, London, 1986).
36. K. D. WEAVER, J. O. STOFFER and D. DAY, *Polym. Comp.* **14** (1993) 515.
37. Y. FU, W. CHEN, M. PYDA, D. LONDONO, B. ANNIS, A. BOLLER, A. HABENSCHUSS, J. CHENG, and B B. WUNDERLICH, *J. Macromol. Sci. Phys.* **B35** (1996) 37.
38. B. W. CHERRY and S. H. TEOH, *Polymer* **22** (1981) 1610.
39. B. W. CHERRY and S. H. TEOH, *ibid.* **25** (1984) 727.
40. J. A. BRYDSON (ed.), ''Plastics materials,'' fourth edition, (Butterworth Scientific, London, 1982).
41. M. HOU, L. YE and Y. W. MAI, *Plast. Rubber Comp. Proc. Appl.* **23** (1995) 279.
42. S. Y. KIENZLE, in ''Polymer blends and alloys, guidebook to commercial products'' (Technomic, Lancaster, PA, 1988).
43. P. Y. B. JAR and R. A. SHANKS, *J. Polym. Sci. Pt B: Polym. Phys.* **34** (1996) 707.

Received 16 June
and accepted 22 July 1998